

Deformable and Posture-Changeable Computational Phantoms and Dosimetry Data for Standard External-Beam Irradiations

Juying Zhang, Yong Hum Na, Aiping Ding, and X. George Xu*

Rensselaer Polytechnic Institute

110 8th St, Troy, NY 12180

xug2@rpi.edu

ABSTRACT

For many radiation dosimetry studies, whole-body phantoms representing workers and patients are used to perform Monte Carlo calculations of organ doses. Since the 1960s, approximately 121 computational phantoms have been reported in the literatures for studies involving ionizing and non-ionizing radiations [1]. There is a barrier currently in developing and in applying person-specific phantoms that are anatomically different from the ICRP reference individuals. We recently adopted the novel-surface modeling method to systematically design a set of pregnant female phantoms by manual work. Now, the automatically algorithm has been systematically developed to develop computational human phantom by all mesh-based organ files. Using this approach we have now developed a pair of mesh-based adult phantoms, RPI-AM and RPI-AF, representing ICRP 89 50th-percentile adult males and adult females. A software has also been developed to develop the phantoms representing different percentile populations and different postures based on this pair of phantoms. The absorbed organ dose results for the external photon exposures using this pair of phantoms were calculated and compared with the ICRP Phantoms. These results demonstrated that, although both sets of phantoms have the same organ volumes and masses, the anatomical differences can cause to dosimetry differences in terms of the effective doses as well as organ absorbed doses. The posture-changing ability has potential applications in many areas of radiation dosimetry.

Key Words: Phantom, Dose, Monte Carlo, Photons

1. INTRODUCTION

Since the 1960s, approximately 121 computational phantoms have been reported in the literatures for studies involving ionizing and non-ionizing radiations [1]. Most of these computational phantoms are based on the Constructive Solid Geometry (CSG) that is simplified in anatomy and difficult to change the shape, size and posture. Increasingly, radiation protection dosimetry requires computational phantoms to realistically represent workers of different body sizes and postures, leading eventually to person-specific dosimetry. A paradigm change in phantom modeling is occurring and the current uncertainty in dosimetry due to the use of single-sized phantoms in an upright standing position will likely be avoided with more advanced methods. A promising new type of phantom geometry, called the Boundary REPresentation (BREP), offers an advantage in comparison with the CSG in the ability to efficiently changing the organ size and shape while preserving the anatomical features.

*Corresponding author

This paper summarizes the development and the application of a pair of reference adult male and female phantoms, RPI Adult Male (RPI-AM) and RPI Adult Female (RPI-AF) that are inherently coupled with mesh-based deformation software algorithms. The organ and body sizes are compatible with the reference data recommended by the International Commission on Radiological Protection (ICRP) [2-4]. This pair of phantoms can also be deformed to match other voxel phantoms. This paper describes the applications of these phantoms to standard external photon beam irradiation conditions for radiation protection dosimetry. Organ absorbed doses and effective doses for these exposures are compared with the other reference adult phantoms.

2. MATERIALS AND METHODS

Figure 1 shows the schematic flowchart of the process of developing deformable whole-body phantoms. The deformation algorithms were implemented in MATLAB® 7.4 to computationally morph the mesh-based original Anatomium™ 3D P1 organ files into two reference adult male and female phantoms whose organs agree within 0.5% with the recommendations of ICRP Publication 23, ICRP Publication 70 and ICRP Publication 89 on organ volume/mass [2-4]. A time-consuming mesh-preprocessing procedure was implemented to improve the quality of the original organ mesh files to correct for “open meshes.” Collision detection algorithm was developed to avoid unwanted surface overlapping. The finalized deformable whole-body mesh-based phantoms (RPI-AM and RPI-AF) were transformed to the solid geometries in the voxel-formatted representation. These whole-body phantoms consist of over 140 deformable organs including their detailed internal anatomical information. These organs are explicitly defined for organ dose calculations using the Monte Carlo methods to define various radiological procedures.

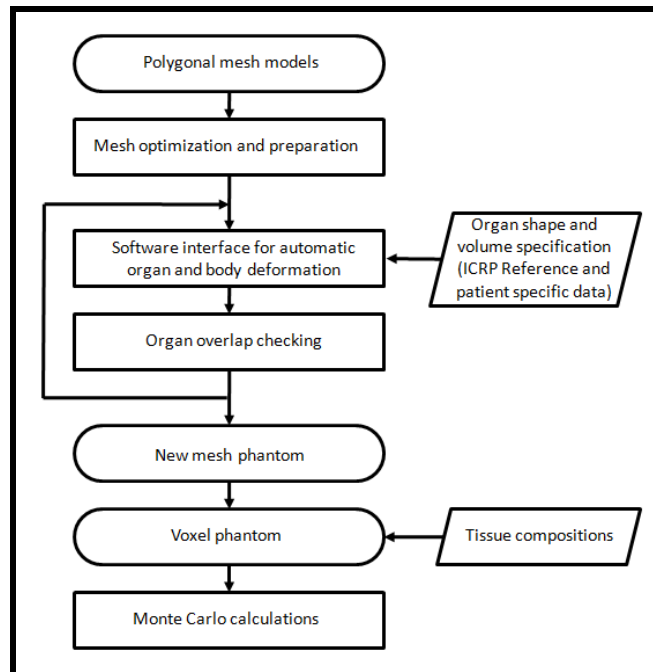


Figure 1 Flowchart of the mesh-based modeling process used to develop adjustable phantoms.

The primary features of these algorithms and tools are summarized as follows:

2.1 Mesh preprocessing

The original Anatomium™ dataset has well-defined human anatomical shapes and structures, but the mesh data structures are defined in a way that is conducive for morphing operations. In order to exploit the entire mesh dataset of an organ while preserving its well-defined anatomy features, it is necessary to preprocess the mesh models by unifying the data structures into a common mesh domain. This is done by making sure that the meshes have unique vertex and face.

2.2 Mesh deformation

A unique scalar multiplication method is mainly used to deform the organ meshes for the elastic deformation of most organ meshes while maintaining both the position and reference volume information. In this method, the entire vertex positions are repositioned along with the direction of each vertex normal. The deformation allows a relative error that the deformed organ mesh volumes matched the ICRP recommended values within 0.5%.

2.3 Mesh collision detection

During the deformation process, all mesh surfaces have to be considered to avoid unwanted mesh overlaps since each mesh-based adult male and female phantoms contains more than 50 organs (i.e., tissues, contents) and 458 bone (i.e., cortex, spongy, cavity) structures. The ray-casting method [5] was used to detect the surfaces in real-time to avoid a collision by examining the distance between two adjacent vertices, as illustrated in Figure 2.

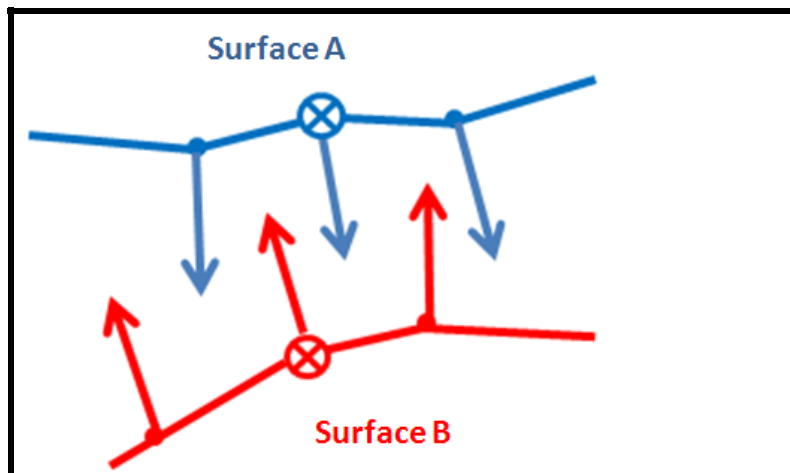


Figure 2 Illustration of the collision detection algorithm for Surfaces A and B represent two organ surfaces. A collision point between two surfaces occurs when the distance between a vertex (labeled as \otimes) to the other surface along the normal direction is less than a pre-determined value. The detection continues until all the vertices on both surfaces have been examined this way.

2.4 Voxelization procedure of the mesh-based geometry to voxel phantoms

For Monte Carlo calculations, a voxelization tool was developed by Visual C++ to convert the mesh-based geometries to voxel-formatted phantoms with the voxel resolution to be specified by a user. The in-house voxelization software is based on parity-counting and ray-stabbing methods for polygonal surfaces that are closed-meshes [6]. The ray-stabbing method is suitable for closed-meshes, but the parity-counting method was also used in this process for certain tissues, such as the vessels and muscles, that are still made of open-meshes. Figure 3 provides a visual inspection of the skeleton before and after the mesh voxelization process.

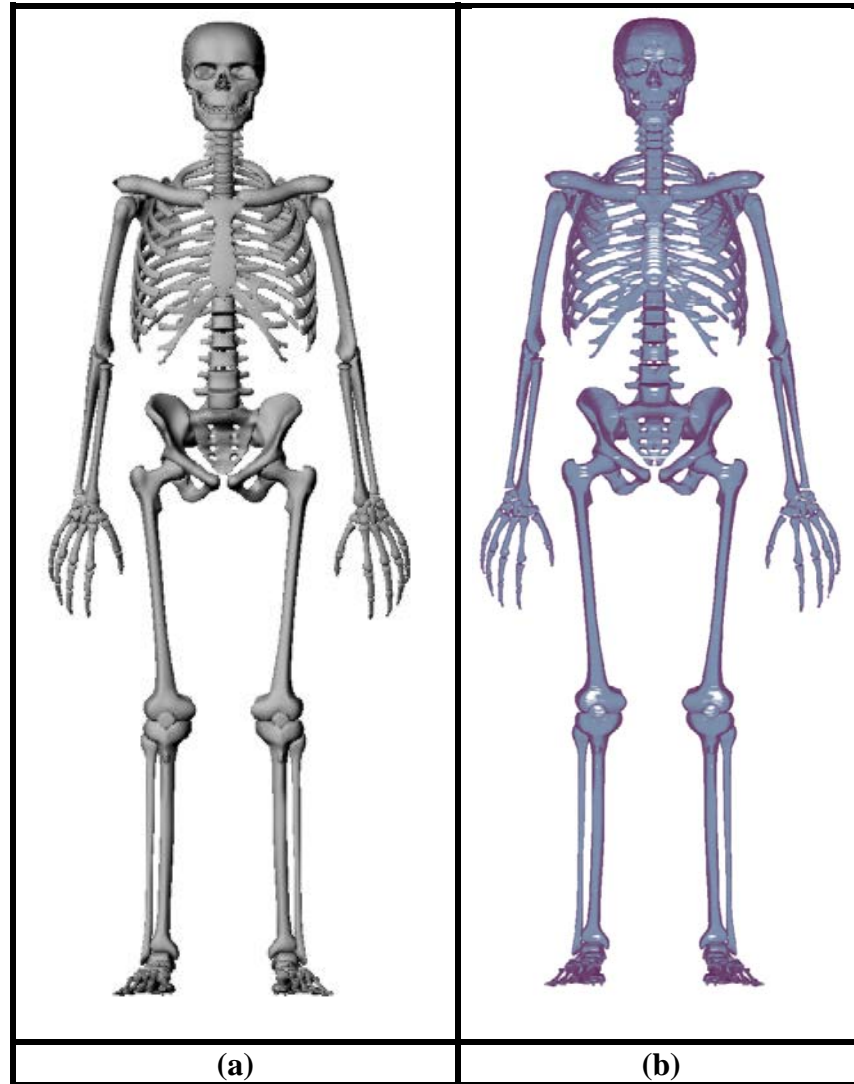


Figure 3 Visual inspection of the male skeleton during the conversion from mesh geometry to voxel geometry showing high fidelity of the process: (a) Mesh format. (b) Voxel format.

2.5 Voxel phantoms setup in MCNPX

For this project, the MCNPX code was used for Monte Carlo calculations [7]. An in-house software is used to create MCNPX input file from the finalized voxel phantom using the standard

“repeated structures” feature. Organ-specific elemental compositions were based on reference values of the ICRP Publication 89. Six standard external source exposure geometries were studied in this project anterior-posterior (AP), posterior-anterior (PA), right lateral (RLAT), left lateral (LLAT), rotational (ROT) and isotropic (ISO). The photon energies range from 10 keV to 10MeV. The MCPLIB04 cross-sectional library for the anatomic interactions based on EPDL 97 evaluation was used. For electron transport, the standard library EL03 was used. The current version of the MCNPX code can handle a maximum of 25 millions of voxels. So during the voxelization process, it is decided to use the 2.7-mm voxel size for RPI-AM phantom and 2.5-mm voxel size for RPI-AF phantom.

2.6 Software development for automatic adjustable phantom

All of the above mesh deformation and voxelization algorithms for the creating of adjustable phantoms were implemented in a software program. The software was developed using the programming language Microsoft® Visual C#. Although the organ volume and overlap were automatically checked during the entire procedures, visual inspections were still necessary. Figure 4 illustrates 3D views of the reference adult male and female phantoms adjusted to match ICRP values. Figure 5 shows the software GUI and the tools in a pull-down menu. These breast deformable phantoms are reported in details elsewhere [8]

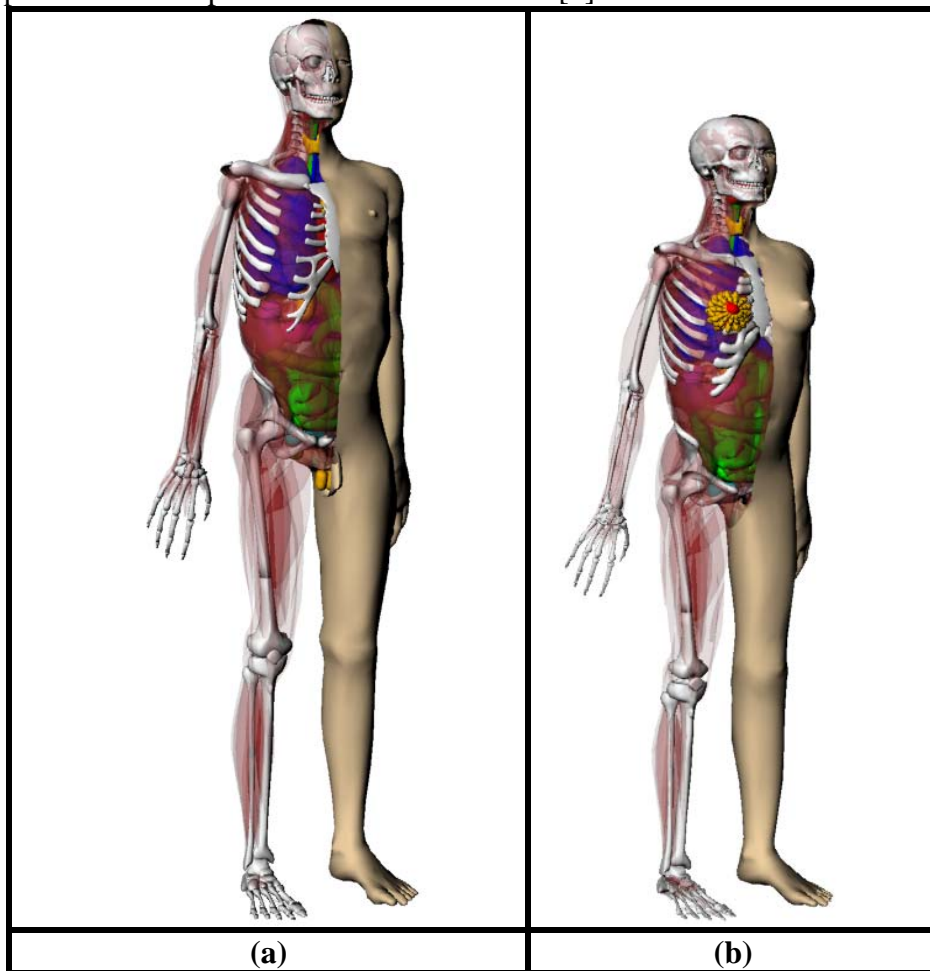


Figure 4 3D frontal and back views of the RPI-AM and RPI-AF phantoms adjusted to match ICRP values. (a) RPI-AM; (b) RPI-AF.

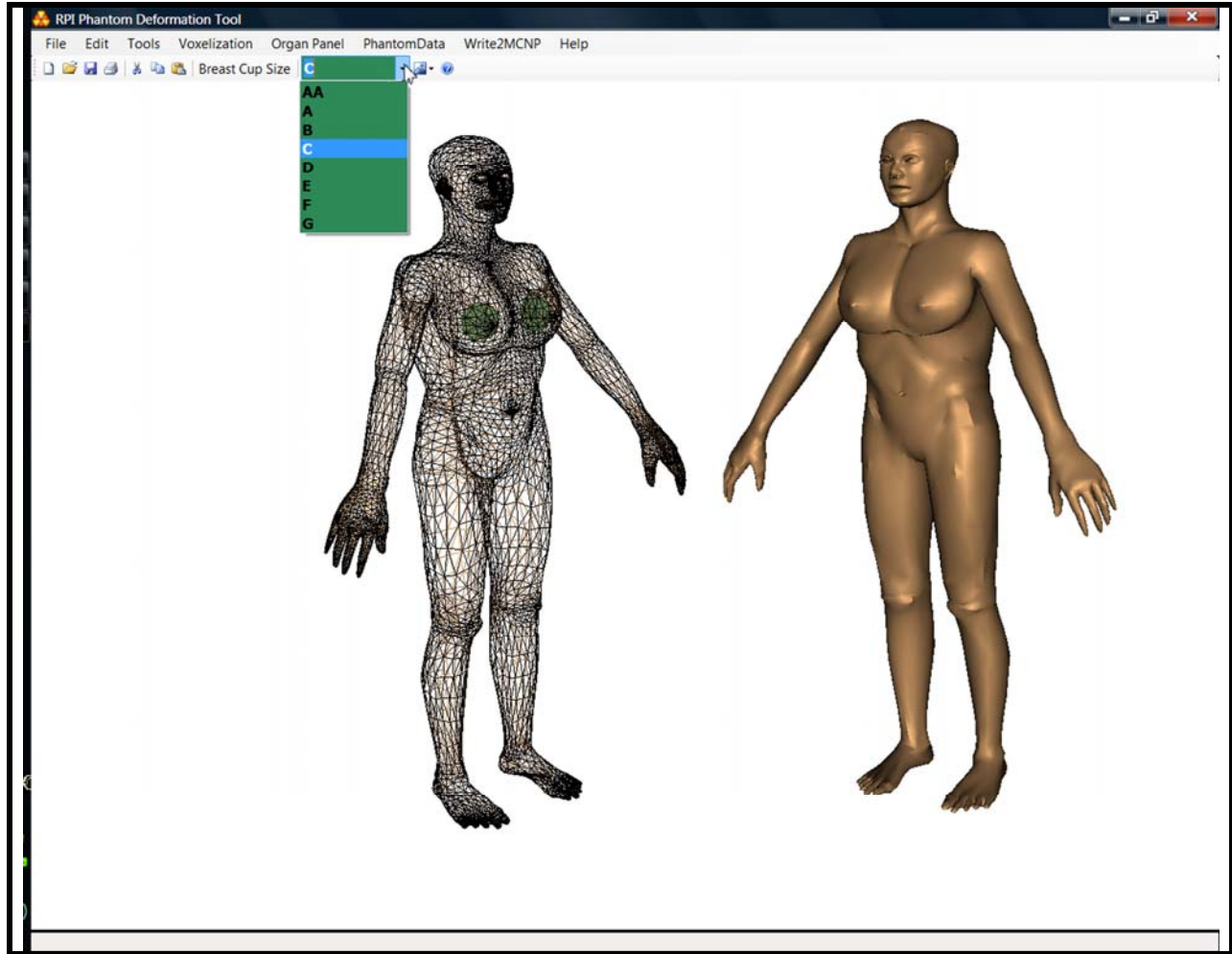


Figure 5 Software GUI for automated adjustable phantom showing various tools and the female phantom of various breast sizes.

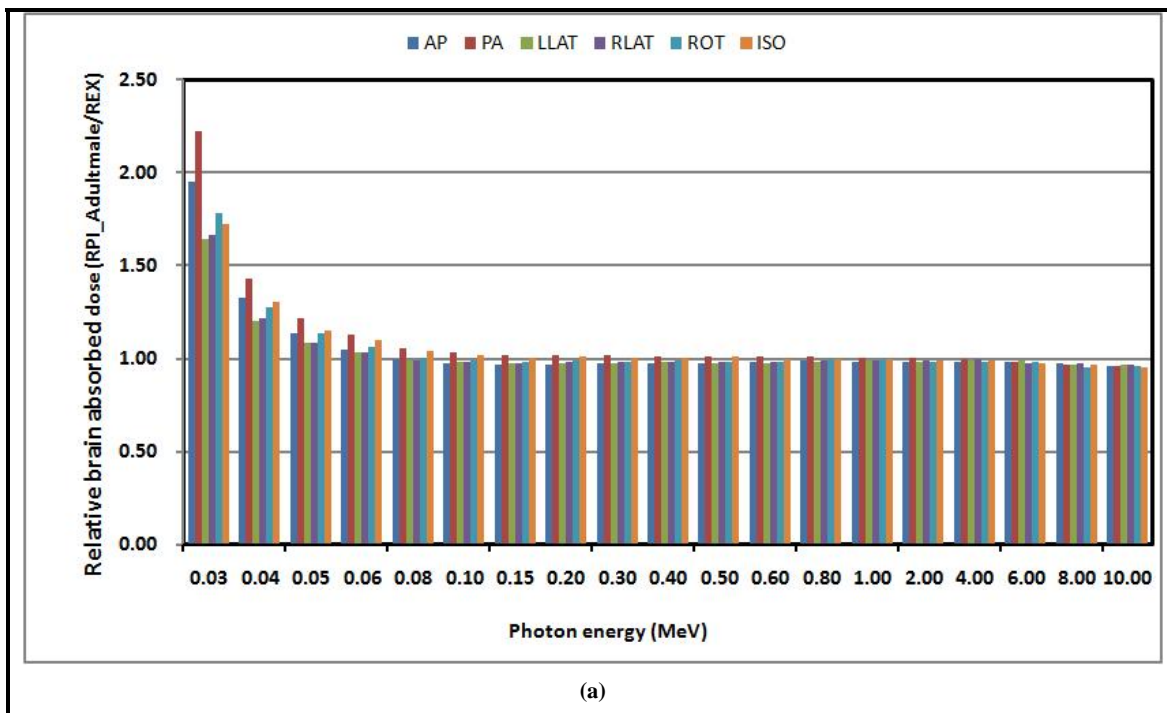
3. Results and Discussion

In this section, we present data on the dose results comparison with those from the ICRP Computational Phantoms, REX and REGINA [9]. The statistical uncertainty of most organ doses is less than 1% (for the eye lens, it is less than 10%). Absorbed doses for the brain are compared with those from the ICRP Phantoms in Figure 6.

The results shown in Figure 6 suggest that, for the brain which is a relatively simple organ, the results from two types of phantoms are very similar for photons whose energy is greater than 0.08 MeV. Since all these phantoms were implemented in a same manner in the MCNPX code, the differences in low energies are due to a combination of anatomy and voxel size (Voxel size of REX is $2.137 \times 2.137 \times 8 \text{mm}^3$). The comparison of the lungs' absorbed doses is shown in Figure 7. There are pronounced differences in these two types of phantoms for photons below 2

Deformable and Posture-changing Computational Phantoms and Dosimetry Data for Standard External-Beam Irradiations

MeV, especially for the lateral irradiations. These differences may be caused by the relative positions of the arm and lungs in these two phantoms. The effective doses of RPI phantoms were also compared with those of ICRP phantoms in Figure 8. Although the effective dose calculations tend to even out the organ dose differences, the comparison suggests that these two types of phantoms differ by about 5% at 1 MeV and up to 50% at 0.01 MeV. From these comparisons, it is clear that these two types of phantoms agree with each other for photons greater than 1 MeV for radiation protection purposes. However, these two types of phantoms yielded rather different organ doses and effective doses for lower photon energies, mainly due to the anatomic differences.



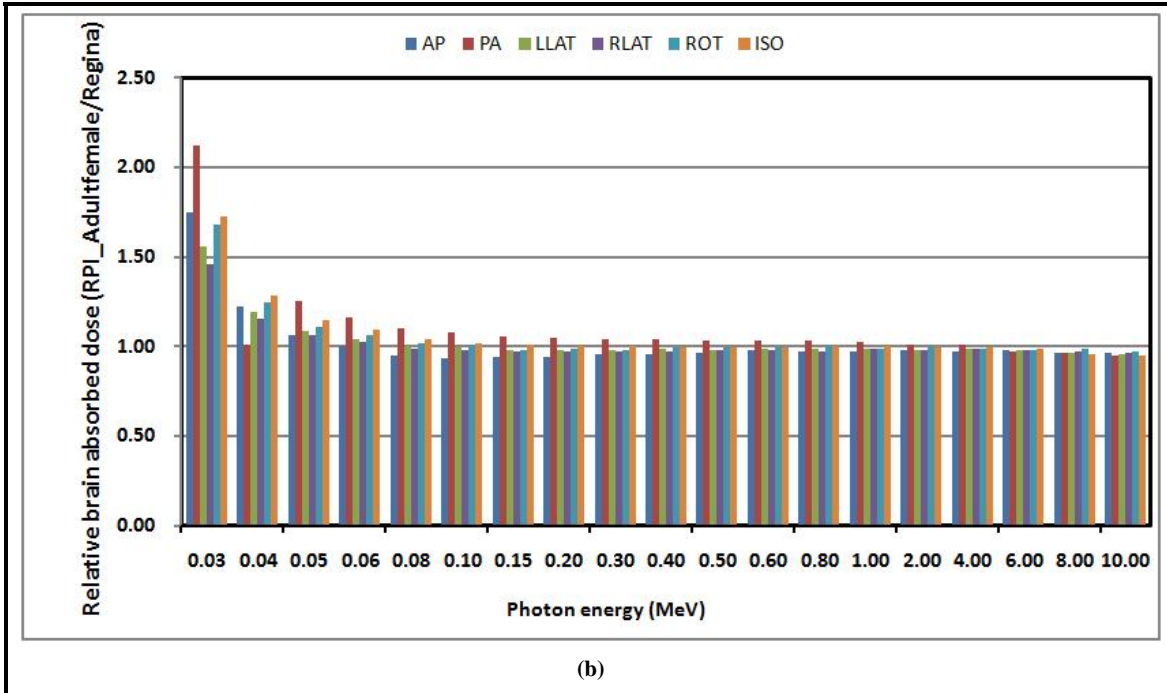
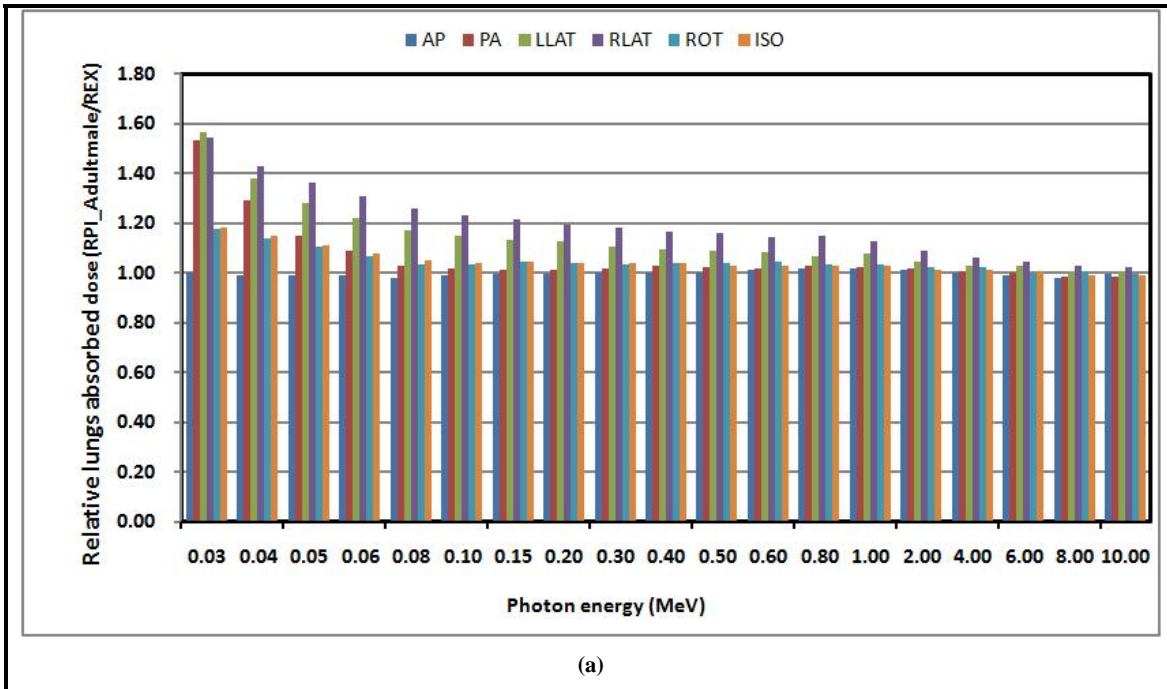


Figure 6. Relative organ absorbed dose compared with the REX/REGINA; (a) relative absorbed doses of the male's brain; (b) relative absorbed doses of the female's brain.



Deformable and Posture-changing Computational Phantoms and Dosimetry Data for Standard External-Beam Irradiations

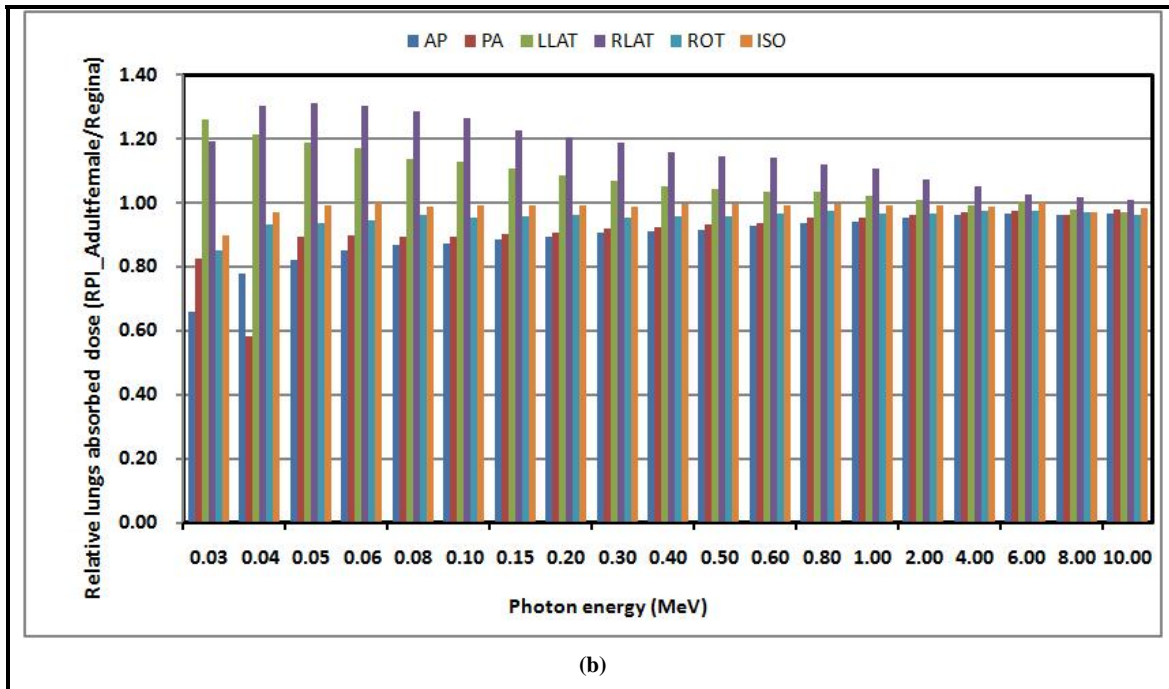


Figure 7. Relative organ absorbed dose compared with the REX/REGINA; (a) relative absorbed dose of male’s lungs; (b) relative absorbed dose of female’s lungs.

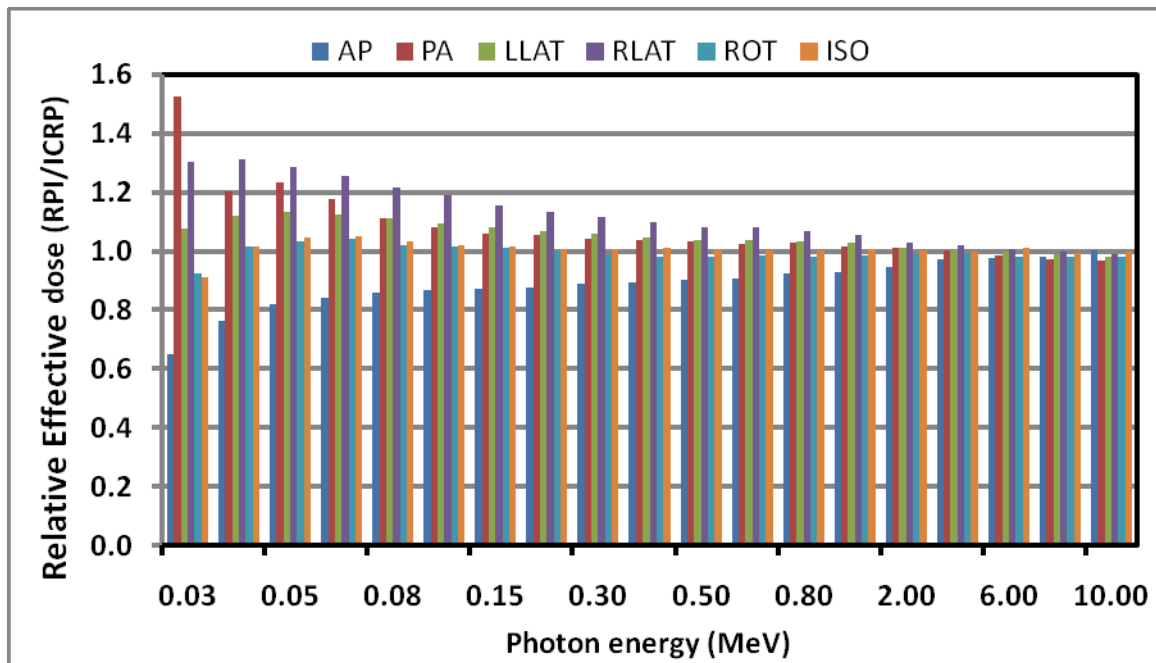


Figure 8. Relative RPI phantom effective dose compared with the ICRP phantoms.

The RPI phantoms were designed to be deformable and posture changeable. To demonstrate the potential usefulness of such phantoms in radiation protection, Figure 9 illustrates several postures developed from the RPI phantoms showing raised arms, walking and sitting. This work is further applied to the assessment of environmental exposure [10].

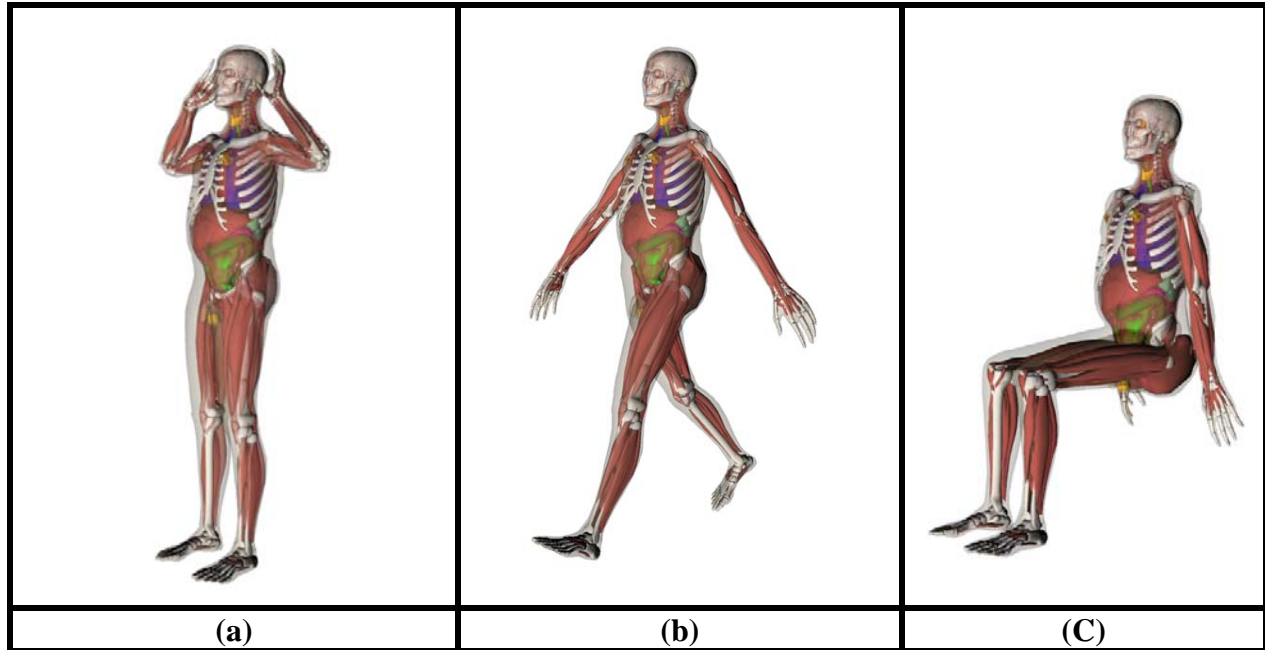


Figure 9 Various postures of size-adjustable phantoms. (a) Raised arms. (b) Walking. (c) Sitting.

4. CONCLUSIONS

In this paper, the efforts to develop and to apply a pair of mesh-based deformable and post-changeable adult male/female phantoms, RPI-AM and RPI-AF, were summarized. The volumes/masses of these phantoms agree with the reference data from ICRP Publications 70 and ICRP Publication 89 with relative errors less than 0.5%. Software has also been developed to apply various operational algorithms. The absorbed organ dose results for the external photon exposures using this pair of phantoms were calculated and compared with the ICRP Phantoms. These results demonstrated that, although both sets of phantoms have the same organ volumes and masses, the anatomical differences can cause to dosimetry differences in terms of the effective doses as well as organ absorbed doses. The posture-changing ability has potential applications in many areas of radiation dosimetry.

ACKNOWLEDGMENTS

The work was supported in part by grants from National Cancer Institute (R01CA116743) and National Library of Medicine (R01LM009362).

REFERENCES

1. Xu XG. "Chapter 1. Computational Phantoms for Radiation Dosimetry: A 40-Year History of Evolution" in "Handbook of Anatomical Models for Radiation Dosimetry" TAYLOR & FRANCIS, 2009 (In print)
2. ICRP 1975 Report of the task group on Reference Man. ICRP Publication 23
3. ICRP. Basic anatomical and physiological data for use in radiological protection: the skeleton. Oxford: Pergamon Press; Ann. ICRP 25(2), ICRP Publication 70; 1995.

Deformable and Posture-changing Computational Phantoms and Dosimetry Data for Standard External-Beam Irradiations

4. ICRP 2002 Basic anatomical and physiological data for use in radiological protection: reference values ICRP Publication 89
5. Amanatides J. and Choi K. Ray Tracing Triangular Meshes, *Proceedings of the Eighth Western Computer Graphics Symposium*, 43–52, 1997
6. Nooruddin F. and Turk G. 2003. Simplification and Repair of polygonal models using volumetric techniques. *IEEE Trans. On Visualization and Computer Graphics* 9(2) 191-205
7. Pelowitz D. B. (2005). MCNPX User's Manual version 2.5.0. Los Alamos National Laboratory Report LA-CP-05-0369
8. Hegenbart L, Na YH, Zhang JY, Urban M and Xu XG. A Monte Carlo study of lung counting efficiency for female workers of different breast sizes using deformable phantoms. *Phys. Med. Biol.* Volume 53, Number 19, 7 October 2008
9. Schlattl H, Zankl M and Petoussi-Henss N. Organ dose conversion coefficients for voxel models of the reference male and female from idealized photon exposures. *Phys. Med. Biol.* (52) 2007 2123–2145
10. Han B, Zhang J, Na YH, Caracappa P, Xu XG. Monte Carlo Modeling of Workers Walking on Contaminated Ground for Accurate Environmental Dosimetry. (submitted to HPS 2009 Annual meeting)